

PROBE-FED RECTANGULAR DIELECTRIC RESONATOR ANTENNAS: THEORETICAL MODELLING & EXPERIMENTS

M. H. NESHATI¹ AND Z. WU²

1: Electrical Dept., Sistan & Baluchistan Univ. Zahedan, Iran.

e-mail: neshat@hamoon.usb.ac.ir

2: Electrical & Electronics Engineering Dept., UMIST,
Manchester M60 1QD, UK.

e-mail: z.wu@umist.ac.uk

ABSTRACT: A Rectangular Dielectric Resonator Antenna (RDRA) is investigated theoretically and experimentally. The Conventional Dielectric Waveguide Model (CDWM) and a numerical method based on the Finite Element Method (FEM) are utilised to calculate the radiation characteristics of the antenna. The results are presented and compared with those obtained by experiments. It is concluded that the CDWM can be used for a first order estimation of the antenna parameters, but more accurate results can be obtained using the FEM for radiation patterns.

Keywords: Dielectric Resonator Antenna, Conventional Dielectric Waveguide Model and Finite Element Method

1. INTRODUCTION

Dielectric Resonators (DRs) using high dielectric constant materials are widely used in shielded microwave circuits such as cavity resonator, filters and oscillators. With an appropriate feed arrangement, they can also be used as antennas and they provide efficient radiation due to extremely low loss in dielectric materials [1-7]. The other advantages of these antennas are: small size, large bandwidth and simple coupling structures in compare to the conventional antennas. Dielectric resonator antennas (DRAs) in cylindrical [1,3], rectangular [2], hemispherical [5] and other geometries [8, 10] have been reported in the literature. Compared with other geometries, rectangular resonators are more attractive for their fabrication advantages, and the existence of two independent aspect ratios for a better design flexibility to obtain impedance matching and radiation requirements. More significantly, in rectangular DRs, mode degeneracy [6] can be avoided by properly choosing the dimensions and hence lower cross polarisation is obtained.

In this paper a probe-fed rectangular DRA, positioned on top of a ground plane, is studied theoretically and experimentally. Two different modelling techniques, namely the Conventional Dielectric Wave-guide Model (CDWM) and the Finite Element Method (FEM) are utilised to predict the radiation parameters of the RDRA including the resonance frequency, radiation patterns, directivity, Q-factor, impedance bandwidth and cross polarisation level.

2. THE CONVENTIONAL DIELECTRIC WAVEGUIDE MODEL (CDWM)

The antenna structure under investigation is shown in Figure 1. The relative dielectric constant of the resonator is ϵ_r and dimensions a , b and h along x -, y - and z -direction respectively. A circular ground plane with a diameter of d supports the DR. A vertically oriented small coaxial probe of height h located at $x=a/2$ and $\phi=0^\circ$ is used to excite the resonator at the dominant mode TE_{111} [6]. For theoretical modelling using the CDWM, as an approximation, the ground plane is considered to be infinitely large. Image theory is then applied and it is removed and the resonator is extended to $z = -h$. The equivalent isolated resonator is fed by a dipole of twice the length of the probe.

Based on the CDWM theory, the isolated resonator is assumed to be the truncation of an infinite rectangular dielectric wave-guide. The field components of the fundamental mode inside the resonator are obtained by solving Maxwell's equations with perfect magnetic wall (PMW) boundary conditions at $x = \pm a/2$ and $z = \pm h$ and continuous tangential fields at $y = \pm b/2$. They are given as:

$$\begin{aligned} E_x &= -(A/\epsilon_d)k_z \cos(k_x x) \cos(k_y y) \sin(k_z z) \\ E_y &= 0 \\ E_z &= (A/\epsilon_d)k_x \sin(k_x x) \cos(k_y y) \cos(k_z z) \end{aligned} \quad (1)$$

$$\begin{aligned} H_x &= (A/j\omega\epsilon_d)(k_x k_y) \sin(k_x x) \sin(k_y y) \cos(k_z z) \\ H_y &= (A/j\omega\epsilon_d)(k_x^2 + k_z^2) \cos(k_x x) \cos(k_y y) \cos(k_z z) \\ H_z &= (A/j\omega\epsilon_d)(k_y k_z) \cos(k_x x) \sin(k_y y) \sin(k_z z) \end{aligned}$$

where $\epsilon_d = \epsilon_0 \epsilon_r$. The characteristic equations for the TE_{111} mode are:

$$k_x = (\mathbf{p}/a), \quad k_y \tan(k_y b/2) = \sqrt{k_x^2 + k_z^2 - k_0^2}, \quad k_z = (\mathbf{p}/2h) \quad (2)$$

and the resonance frequency is the solution of the separation equation given by:

$$k_x^2 + k_y^2 + k_z^2 = \epsilon_r k_0^2 \quad (3)$$

where k_0 is the free space wave number.

The radiation fields are considered to be due to the equivalent magnetic currents on the surfaces of the resonator. In far field region, the field components are

$$\begin{aligned} E_q &\approx -\frac{jk_0 e^{-jkr}}{4\pi r} L_f, \quad E_f \approx +\frac{jk_0 e^{-jkr}}{4\pi r} L_q \\ H_q &= +\frac{E_q}{h_0}, \quad H_f = -\frac{E_f}{h_0} \end{aligned} \quad (4)$$

It can be shown that

$$L_f = \left(\frac{2A\mathbf{p}^2}{\mathbf{e}_d ah} \right) \cdot \cos \mathbf{f} \cos(k_0 \frac{a}{2} \sin \mathbf{q} \cos \mathbf{f}) \cos(k_0 h \cos \mathbf{q}) \left\{ \frac{D_1}{D_2} + \frac{2D_1}{D_3} \right\} + \left(\frac{2Ak_0 k_x \mathbf{p}}{\mathbf{e}_d h} \right) \cdot \cos(\mathbf{dp}/2) \cdot \sin \mathbf{q} \sin(2\mathbf{f}) \sin(k_0 \frac{b}{2} \sin \mathbf{q} \sin \mathbf{f}) \cdot \cos(k_0 h \cos \mathbf{q}) \cdot \cos(k_0 \frac{a}{2} \sin \mathbf{q} \cos \mathbf{f}) \cdot \frac{1}{D_2 \cdot D_3}$$

and

$$L_q = \left(\frac{2A\mathbf{p}^2}{\mathbf{e}_d ah} \right) \cos \mathbf{q} \sin \mathbf{f} \cos(k_0 \frac{a}{2} \sin \mathbf{q} \cos \mathbf{f}) \cdot \cos(k_0 h \cos \mathbf{q}) \frac{D_1}{D_2} + \left(\frac{2A\mathbf{p}k_0 k_x}{\mathbf{e}_d h} \right) \cos(\mathbf{dp}/2) \sin 2\mathbf{q} \cos^2 \mathbf{f} \cdot \sin(k_0 \frac{b}{2} \sin \mathbf{q} \sin \mathbf{f}) \cdot \cos(k_0 h \cos \mathbf{q}) \cos(k_0 \frac{a}{2} \sin \mathbf{q} \cos \mathbf{f}) \frac{1}{D_2 \cdot D_3}$$

with

$$D_1 = \left(\frac{\sin(k_0 \frac{b}{2} \sin \mathbf{q} \sin \mathbf{f} + \mathbf{dp}/2)}{k_0 \sin \mathbf{q} \sin \mathbf{f} + \mathbf{dp}/b} + \frac{\sin(k_0 \frac{b}{2} \sin \mathbf{q} \sin \mathbf{f} - \mathbf{dp}/2)}{k_0 \sin \mathbf{q} \sin \mathbf{f} - \mathbf{dp}/b} \right)$$

$$D_2 = (\mathbf{p}/2h)^2 - (k_0 \cos \mathbf{q})^2, D_3 = (\mathbf{p}/a)^2 - (k_0 \sin \mathbf{q} \cos \mathbf{f})^2$$

The directivity of the antenna can be calculated using the equation given by:

$$D_{\max} = \frac{(E_q^2(\mathbf{q}, \mathbf{f}) + E_f^2(\mathbf{q}, \mathbf{f}))_{\max}}{\frac{1}{4\mathbf{p}} \int_0^{2\mathbf{p}} \int_0^{2\mathbf{p}} (E_q^2(\mathbf{q}, \mathbf{f}) + E_f^2(\mathbf{q}, \mathbf{f})) \sin \mathbf{q} \mathbf{q} \mathbf{f} d\mathbf{q} d\mathbf{f}} \quad (5)$$

The Q-factor of the RDRA is defined as

$$Q_0 \approx Q_r = \mathbf{w}W/P_r$$

where w is the stored energy inside the resonator and P_r is the total radiated power by the RDRA, which are given respectively by:

$$W = \frac{A^2}{32\mathbf{e}_d} abh \left(1 + \frac{\sin(k_y b)}{k_y b} \right) (k_x^2 + k_z^2), \quad P_r = \frac{1}{4} \frac{1}{h_0} \int_0^{2\mathbf{p}} \int_0^{2\mathbf{p}} (|E_q|^2 + |E_f|^2) r^2 \sin \mathbf{q} d\mathbf{q} d\mathbf{f} \quad (6)$$

For Q-factor measurement, the unloaded Q-factor, Q₀, of the RDRA can be obtained using the one port reflection coefficient measurement discussed in [11] and the impedance bandwidth of the RDRA (VSWR ≤ 2.6) is approximately related to the Q₀ factor by:

$$BW(\%) \approx (100/Q_0)$$

3. THE FINITE ELEMENT MODEL

The RDRA in Figure 1 is numerically investigated using the HP85180A High Frequency Structure Simulator (HFSS) [12]. The HFSS is a software package based on the FEM. In general, in the HFSS, the geometric model is divided into a large number of elements, which are tetrahedra. The value of a vector field quantity such as **E**- or **H**-field inside each element

is obtained by interpolation from the vertices of the tetrahedron. The antenna structure is surrounded by an absorbing sphere with the second order radiation boundary condition given by [12]:

$$(\nabla \times \mathbf{E})_{\tan} = jk_0 \mathbf{E} - (j/k_0) \nabla_{\tan} \times (\nabla_{\tan} \times \mathbf{E}) + (j/k_0) \nabla_{\tan} (\nabla_{\tan} \cdot \mathbf{E}) \quad (7)$$

where \mathbf{E}_{\tan} is the tangential component of the \mathbf{E} -field on the surface. The absorbing sphere is placed at least a quarter of wavelength away from the source of the signal. The HFSS then maps the \mathbf{E} -field computed in (4) on the absorbing surface and calculates the far-field and radiation patterns using

$$\mathbf{E}(x, y, z) = \int_s [(j\omega\mu_0 \mathbf{E}_{\tan})\mathbf{G} + (\mathbf{E}_{\tan} \times \nabla \mathbf{G}) + (\mathbf{E}_{normal} \times \nabla \mathbf{G})] ds \quad (8)$$

where $\mathbf{E}_{\tan}, \mathbf{H}_{\tan}$ are the tangential components of electric and magnetic fields respectively and \mathbf{E}_{normal} is the normal component of the electric field on the radiation surface s , and \mathbf{G} is the free space Green's Function.

4. RESULTS

For a specific dielectric resonator with $a=19\text{mm}$, $b=19\text{mm}$, $h=9.5\text{mm}$ and $\epsilon_r=38$ supported by a circular ground plane with $d=\infty$ and $d=10\text{cm}$, the results of theoretical and numerical analysis are listed in Table 1, together with their corresponding measured values for $d=10\text{cm}$. The radiation patterns for $d=\infty$ and $d=10\text{cm}$ are shown in Figures 2 and 3 respectively.

It can be seen that, for $d=\infty$ the predicted radiation patterns using the CDWM and HFSS agree very well. Also the predicted directivity agrees well with an error of 10%. The predicted resonance frequency using the CDWM is less than that of the FEM with only 1.5% difference. The simulated Q-factor, using the HFSS, differed from the CDWM ones by +12% and so, the BW predicted value is lower by the same factor.

In case of the finite ground plane, it can be observed that there is only a difference in simulated and measured E-Plane radiation patterns compared with the CDWM at small elevation angles near the ground plane. This is believed to be due to the effect of the finite size of the ground plane. As a result the numerical method produces more accurate radiation patterns. The simulated result for the directivity has not such good agreement compare to the experiment where the error can be high as +28.5%. It is said that this error is due to the non-convergence of the numerical method in the allowed run time of the simulation. However, the CDWM has more accurate result for the directivity. The predicted resonance frequency and Q-factor using the HFSS in this case have an error of -5% and +19% respectively in compare to measured ones. These errors are because of the existence of thin air gaps between the RDRA and ground plane and between the RDRA and the feed probes, which are not included in the simulation. The difference between measured and simulated cross-polarisation level is 12.5dB.

5. CONCLUSIONS

Two different modelling methods are used for the modelling of a rectangular DRA. Results indicate that the CDWM predicts a first order estimation of the RDRA radiation parameters and the HFSS can produce more accurate radiation patterns. However, the radiation patterns are affected by the finite size of the ground plane at small angles near to the ground plane. Also there is an error in the simulated resonance frequency and Q-factor in compare to the experimental results case of finite ground plane. The effects of finite size of ground plane and air gaps in the antenna structures need to be taken into consideration in the theoretical

modelling to produce more accurate prediction of radiation parameters, in which case the CDWM has its limitation.

6. REFERENCES

- [1] Long S. T., McAllister M. W. and Shen L. C., "The Resonant Cylindrical Dielectric Cavity Antenna", IEEE Transactions on Antenna & Propagation, Vol. AP-33, 1983, pp. 406-412.
- [2] M. W. McAllister, S. A. Long And G. L. Conway, "Rectangular dielectric resonator antenna", Electronics Letters, Vol. 19, 1983, pp. 218-219.
- [3] G. Drossos, Z. Wu, and L.E. Davis, "Cylindrical dielectric resonator antennas: theoretical modelling and experiments", Microwave & Communication Technologies Conference (M&RF'97), Wembley Conference Centre, London, UK, pp. 34-39.
- [4] R. K. Mongia, and P. Bhartia "Dielectric resonator antenna - A Review and general design relations to resonant frequency and bandwidth", International Journal of Microwave and Millimetre-Wave Computer Aided Engineering, Vol. 4, 1994, pp. 230-247.
- [5] M. W. McAllister and S. A. Long, "Resonant Hemispherical Dielectric Antenna", Electronics Letters, vol. 20, pp. 657-659, 1984.
- [6] R. K. Mongia, and A. Ittipiboon, "Theoretical and experimental investigations on rectangular dielectric resonator Antennas", IEEE Transaction on Antenna and Propagation, Vol. AP-45, 1997, pp. 1348-1356.
- [7] Petosa, A. Ittipiboon, Y. M. M. Antar, D. Roscoe and M. Cuhaci, "Recent advances in dielectric resonator antenna technology", IEEE Transaction on Antenna and Propagation Magazine, Vol. 40, 1998, pp. 35-48.
- [8] R. K. Mongia, A. Ittipiboon, P. Bhartia, and M. Cuhaci, "Electric Monopole Antenna Using a Dielectric Ring Resonator", Electronics Letters, vol. 29, pp. 1530-1531, 1993.
- [9] R. K. Mongia, A. Ittipiboon, Y. M. M. Antar, P. Bhartia, and M. Cuhaci, "A Half Split Cylindrical Dielectric Resonator Antenna Using Slot Coupling", IEEE Microwave and Guided Waves Letters, vol. 3, pp. 38-39, 1993.
- [10] M. T. K. Tam and R. D. Murch, "Compact Circular Sector and Annular Sector Dielectric Resonator Antennas", IEEE Transactions on Antennas & Propagation, vol. 47, pp. 837-842, 1999.
- [11] Z. Wu, and L.E. Davis, "Automation-oriented technique for quality-factor measurement of high- T_c super-conducting resonators", IEE Proceedings Science and Measurement Technology, Vol. 141, No. 6, 1994, pp 527-530.
- [12] Hewlett-Packard Company, "HP85180A High-Frequency Structure Simulator (HFSS): User's Reference", 1994.

Table 1. Radiation characteristics of the RDRA on a circular ground plane.

Parameter	CDWM $d=\infty$	FEM		Measured $d=10\text{cm}$
		$d=\infty$	$d=10\text{cm}$	
Frequency (GHZ)	2.022	2.053	2.078	2.175
Q-Factor	33.088	37.185	36.793	30.906
Bandwidth (VSWR<2.6) (%)	2.850	2.551	2.578	3.075
Directivity or Gain	2.881	3.198	4.629	3.344
Cross-Polarisation level (dB) at $\theta=0^\circ$	–	–	33.959	21.425

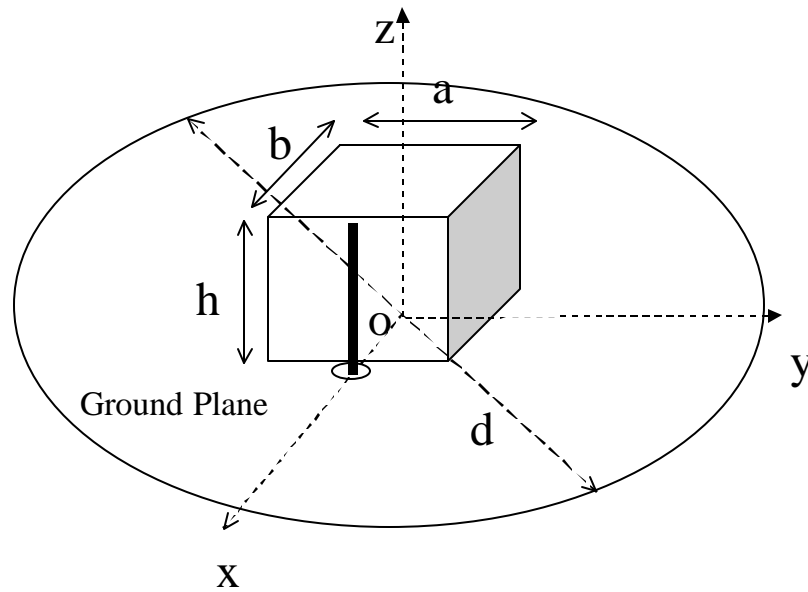


Figure 1: The structure of the RDRA under investigation

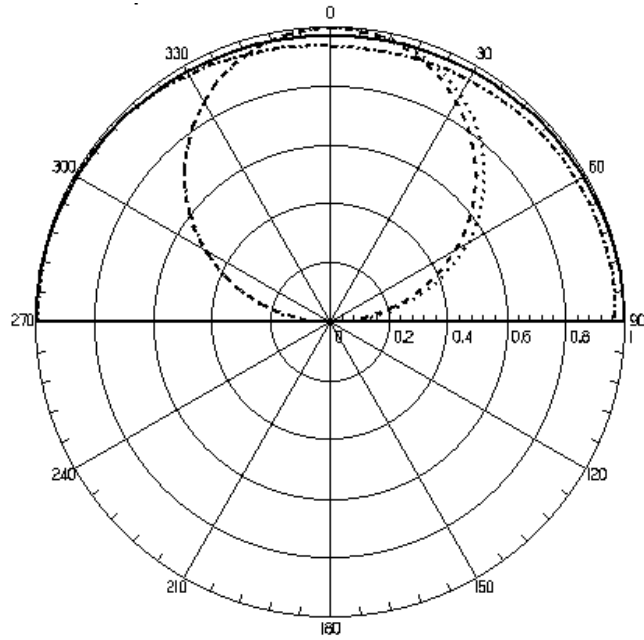


Figure 2: Theoretical co-polarisation radiation patterns of the RDRA on an infinite ground plane.

(CDWM: ——— E_θ at $\phi=0^\circ$ - - - - - E_θ at $\phi=90^\circ$)
 (FEM: - · - · - E_θ at $\phi=0^\circ$ ······· E_θ at $\phi=90^\circ$)

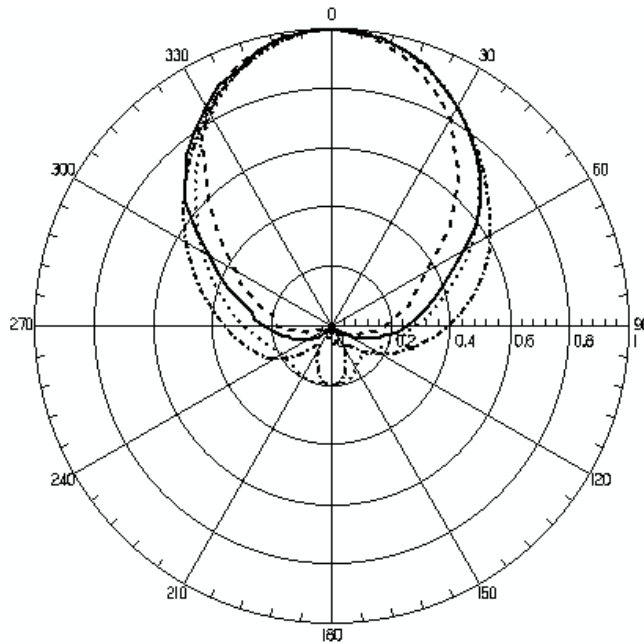


Figure 3: Theoretical and measured co-polarisation radiation patterns of the RDRA on a finite circular ground plane $d=10\text{cm}$.

(Measured: ——— E_θ at $\phi=0^\circ$ - - - - - E_θ at $\phi=90^\circ$)
 (FEM: - · - · - E_θ at $\phi=0^\circ$ ······· E_θ at $\phi=90^\circ$)